Modeling topsoil carbon sequestration in two contrasting crop production to set aside conversions with RothC – calibration issues and uncertainty analysis

Fotini E. Stamati[*a], *Nikolaos P. Nikolaidis*[a], *Jerald P. Schnoor*[b]

[a]Department of Environmental Engineering, Technical University of Crete (TUC), University Campus, 73100, Chania, Greece. [b]Department of Civil and Environmental Engineering, 4105 Seamans Center, The University of Iowa, Iowa City, Iowa 52242

*corresponding author, Tel:+302821037831; Fax:+302821037847;
e-mail: fotini.stamati@enveng.tuc.gr

ABSTRACT

Model simulations of soil organic carbon turnover in agricultural fields have inherent uncertainties due to input data, initial conditions, and model parameters. The RothC model was used in a Monte-Carlo based framework to assess the uniqueness of solution in carbon sequestration simulations. The model was applied to crop production to set aside conversions in Iowa (sandy clay-loam soil, humid-continental climate) and Greece (clay-loam soil, Mediterranean). The model was initialized and calibrated with particulate organic carbon data obtained by physical fractionation. The calibrated values for the Iowa grassland were 5.05 t C ha^{-1}, 0.34 y^{-1}, and 0.27 y^{-1} for plant litter input and decomposition rate constants for resistant plant material (RPM) and humus, respectively, while for the Greek shrubland these were 3.79 t C ha^{-1}, 0.21 y^{-1}, and 0.0041 y^{-1}, correspondingly. The sensitivity analysis revealed that for both sites, the total plant litter input and the RPM rate constant showed the highest sensitivity. The Iowa soil was projected to sequester 17.5 t C ha^{-1} and the Greek soil 54 tC ha^{-1} over 100 years and the projected uncertainty was 65.6% and 70.8%, respectively. We propose this methodology to assess the factors affecting carbon sequestration in agricultural soils and quantify the uncertainties.

Keywords: C/N sequestration, aggregation, particulate OM, RothC modeling, calibration, uncertainty

1. Introduction

Conversion of native vegetated lands to croplands is known to induce soil organic matter (SOM) losses due to ploughing. In medium to fine textured, structured soils, during ploughing, aggregates are partly destroyed and physically protected SOM is exposed, the bio-available fraction becomes then bio-accessible and can be microbially oxidized causing SOM decline and consequent CO_2 emissions (Balesdent et al., 1998). Most of the SOM loss, in structured soils, is attributed to the destruction of large macro-aggregates which consist primarily of labile SOM (Emadi et al., 2009). The free or occluded labile (light fraction with a density lower than 1.6-2 g cm^{-3}) SOM, consisting primarily of particulate organic matter (POM), is the fraction mostly affected by ploughing (Wagai et al., 2008), while the denser mineral fraction is mostly affected in the medium- to long-term time scale (Don et al., 2009). POM, unprotected though, is also most affected due to ploughing in structurelless sandy soils.

On the other hand, the conversion of cultivated fields to grasslands, shrublands or forests has been shown to sequester carbon in soils (Guo and Gifford, 2002), which is primarily as attributable to POM changes in the topsoil (Potter and Derner, 2006). Soussana et al (2004) have reported that it takes twice as long to restore the carbon content in restored grasslands compared to the time it takes to lose the carbon through cultivation (i.e. ploughing). The re-formation of soil aggregates after such land use change indicates the ‘soil resilience’ potential (Lal, 1997). Particle aggregation provides structure to soils and has been related to soil fertility. An “agronomically valuable” soil is a soil where greater than 60% of the particle mass is in the range between 0.25 and 10 mm (Banwart et al., 2011). The extent of soil degradation and restoration depends on management practices as well as the factors that determine soil structure and aggregation (Angers and Carter, 1996) which includes SOM content, soil mineralogy, and clay content, soil macrofauna (e.g. earthworms), and root, root hair and (vesicular-arbuscular) mycorrhizal hyphal densities, as well as the climate under which the soil was formed. Understanding the factors controlling land use effects on soil particle aggregation is therefore very important in order to improve SOM modelling and soil restoration techniques (Rees et al., 2005; Angers and Carter, 1996). Physical fractionation schemes can be used to appraise the effect of land use change on particle aggregation and estimate the fractions of carbon such as the humus and particulate fractions that can be used to calibrate the turnover of carbon with mathematical models.

The turnover of SOM is usually described with multi-compartment models. Many soil carbon models have been utilized in the scientific literature and comparison of their structure and modeling results can be found in review papers (e.g. Nikolaidis and Bidoglio 2011; Battle-Aguilar et al., 2010; Manzoni and Porporato, 2009; Smith et al., 1997; Shibu et al., 2006; Fallon and Smith, 2000). These models have been used to simulate SOM turnover of discrete soil organic carbon pools using either default or calibrated decomposition rate constants mostly without accounting for the uncertainty that arises from the initial conditions, model parameters, inputs and model structure with very few exceptions (Juston et al., 2010; Paul et al., 2003). However, models can be greatly constrained by using field measured carbon pools to initialize and calibrate the model. For example physical fractionation schemes like dispersing and sieving (Krull et al., 2005) as well density fractionation (Zimmermann et al., 2007) have been used to measure modeled carbon pools in RothC carbon model. The complexity of the interrelationships among the carbon turnover model parameters and inputs require a modeling framework to assess the uniqueness of solution and the uncertainties due to model structure, initial conditions, model parameters and input data.

The objective of this study was twofold: a) develop a procedure for model parameter estimation applied to cases of cropland to fallow conversions (through initialization and calibration with field derived physical fractionation data) where the litter/manure input has not been measured and b) quantify the uncertainties in RothC modeling results.

2. Methodology

A Microsoft Excel version of the Rothamsted Carbon Model-version RothC-26.3 (Coleman and Jenkinson, 1999) was developed and used in conjunction with a statistical simulation package @RISK (PALISADES Corp.) in order to simulate the uncertainty in topsoil carbon turnover during cropland to set aside from crop production (which was cultivated in the past and was left uncultivated with native vegetation) conversion in Iowa (grassland) and Greece (shrubland). Field data derived by a physical fractionation scheme were used to initialize and calibrate the model.

2.1. Study sites

Two sites were chosen with paired plots of adjacent cropland and set aside fields. The first site (indicated as IA) was Iowa City, IA, USA (41°45´N, 91°44´W, 230 m), indicative of humid continental climate with soils with coarse texture-sandy loam. Mean annual temperature in the region is 10 ^{o}C (21.6±3.1 ^{o}C, MAY – SEP) and mean annual precipitation 923 mm (60%, MAY - SEP). The second site (indicated as GR) was in the northern part of Chania Perfecture, Crete, Greece (39°25´N, 51°41´E, 10 m), where typical semi-arid, Mediterranean climate dominates and soils have finer texture-clay loam. Mean annual temperature in the region is 18 ^{o}C (12.5±3 ^{o}C, NOV – MAR) and mean annual precipitation 652 mm (82%, NOV-MAR). Although, during the winter period in Iowa soil is covered by snow there is a long wet and warm cropping period from May to September, while in Greece most of the precipitation is taking place during the winter time, from November to March where the temperature is low and therefore warm cropping period is dry.

Soils in both sites were recent alluvial depositions. Iowan soils were very deep, poorly drained soils, formed in colluvium alluvial fans, and characterized as colo-ely (Udolls Mollisols or Phaeozems-FAO, 1998). Udolls are more or less freely drained Mollisols of humid climates that naturally were tall grass prairies and are used as croplands. Cretan alluvial deposits (Quartenary formations) are shallower than those at Iowa and characterized as calcaric Regosols-known also as para-rendzinas, or Entisols in the American System (FAO, 1998). Regosols are frequently associated with Leptosols and Arenosols and are soils with very limited soil development. Regosols and Phaeozems are used as arable lands and correspond to 7.1% and 9.7% of the total world area used for arable cultivation (which is 18 % of total world land cover) (The World Factbook, 2008).

The Iowa arable field was disk plowed to about 30 cm soil depth and used for the production of corn and soybeans. Prior to being set-aside, about 20 years ago, the Iowa uncultivated field received the same management. Mollisols in the Midwest have been cultivated for more than 150 years. However, most of the organic matter decline occurred by the 1960 and has been at steady state under production practices in place since then (David et al., 2009). The Greek arable field was used for the production of green vegetables and tillage was lighter and shallower compared to Iowa. The Greek field had been set aside from crop production about 35 years. For modelling purposes, the soils have been assumed to be at steady state in terms of carbon content, however this assumption is inherently uncertain.

Soil sampling was designed based on the objective to simulate the evolution of soil carbon from cultivation to set aside conditions. Most of the changes in aggregation and SOM storage are known to take place in the topsoil due to plant rooting depth (Potter and Derner, 2006). Typical rooting depth of Mediterranean shrublands found in Greece was 10 cm (Beier et al., 2009). Organic carbon has been found to concentrate in the top 10 cm and a sharp decline has been observed n the subsoil of both tilled (2.1±0.5 times) and no tilled (1.6±0.3 times) fields of olive groves in the alluvial plain of Koiliaris River Basin (Fig. S1 in the supporting information, data taken from the 'soiltrec' project (www.soiltrec.eu) field campaign). On the other hand although the rooting depth in Iowa grassland is deeper most of the root biomass is found in the topsoil. Studies have indicated that 73-87% of the total root biomass (0-125 cm) across different plants in Iowa was found in the 0-35 cm (Tufekcioglu et al., 2003), while 90% of prairie root biomass (0-50 cm) was found in the 0-25 cm and 60% in the upper 5-cm (Buyanovsky et al., 1987). In order to compare the results between Greece and Iowa, surface soil was sampled from 0-10 in both croplands and set aside fields. Each sample was a composite of five representative subsamples. Bulk density was calculated using 100 cm^3 cores. The 10-30 cm soil depth was also sampled from the Iowa soils in order to account for the greater rooting depth and validate the changes in total SOM storage. Recent plant residues and stones were removed from the fresh soil samples by hand. The samples were air dried and stored in a cool-dry place not more than 2-3 months until further analysis. Subsoil samples were measured for SOM content and bulk density.

2.2. Physical fractionation

The methodological approach was based on a physical fractionation scheme (Fig. S2 in the supporting information) described in detail in the supporting information material. Briefly, the soils were separated into five (slake resistant) water stable aggregate (WSA) fractions according to the procedure based on Elliott (1986): i) large macro-aggregates (>2000 μm), ii) medium macro-aggregates (1000-2000 μm), iii) small macro-aggregates (250-1000 μm), iv) micro-aggregates (53-250 μm), and v) silt-clay sized micro-aggregates and minerals (<53 μm). Mean weight diameter (MWD) was also calculated as an index of aggregate stability. In order to reveal possible differences in the composition and turnover rates of the macro-aggregates of different sizes and the patterns of the decomposition sequence the microaggregate isolation procedure outlined in Lichter et al., (2008) was applied to both small macro-aggregates (250-1000 μm) and composite macro-aggregates (>250 μm) samples. Sub-samples of these aggregates were separated into the following fractions: i) coarse particulate organic matter and sand (cPOM: >250 μm), ii) micro-aggregates (mM: 53-250 μm), and iii) easily dispersed silt-clay fractions (sc-M <53 μm). The mM fraction as well 53-250 μm sized aggregates (micro-aggregates) were further separated to fine particulate organic matter and sand (fPOM: 53-250 μm) and silt-clay fraction of the micro-aggregate (sc-mM <53 μm). All fractions were measured for their content in C and N.

Analytical methods used for the physicochemical soil characterization and further soil characteristics are presented in the supporting information material.

2.3. Carbon turnover modeling

A Microsoft Excel version of the Rothamsted Carbon Model-version RothC-26.3 (Coleman and Jenkinson, 1999) was developed. An initial excel version was provided to us by Todorovic et al (2010). The calculation of RothC ‘abc’ parameters (described in the following paragraph) was added in the excel version we developed. The model was crossed verified with the original exe of RothC-26.3 (Coleman and Jenkinson, 1999) with the default values of model parameters and gave identical results. No structural changes were made.

RothC is based on a monthly time step calculation and can simulate SOC turnover over a period ranging from a few years to a few centuries. Soil organic carbon is split into four active pools which decompose by a first-order process with its own characteristic rate and an amount of inert organic matter (IOM) resistant to decomposition. The four active compartments are Decomposable Plant Material (DPM), Resistant Plant Material (RPM), Microbial Biomass (BIO) and Humified Organic Matter (HUM). The model default decomposition rate constants (k, years^{-1}) for each compartment are: DPM: 10.0, RPM: 0.3, BIO: 0.66, and HUM: 0.02. The decomposition rate constants are corrected by a rate modifying factor for temperature (a), the topsoil moisture deficit rate modifying factor (b), and the soil cover factor (c). The model apportions plant litter input between DPM and RPM using the factors reported by Coleman and Jenkinson (1999); i.e. 1.44 for grassland and 0.67

for shrubland. Both DPM and RPM decompose to form CO_2, BIO and HUM. The proportion that goes to CO_2 and to BIO and HUM is determined by the clay content of the soil. The BIO and HUM is then split into 46% BIO and 54% HUM. BIO and HUM both decompose to form more CO_2, BIO and HUM.

The meteorological data used in the modeling exercise (average monthly mean temperature, precipitation, and open pan evaporation) were obtained by the Local Climate Estimator (New LocClim 1.10, 2006) and are presented in Table S1 in the supporting information material. Soil thickness was set to 10 cm. The set-aside fields were covered the whole year by grass (IA) and shrubs (GR). Field measured SOC and POM content, derived by the applied physical fractionation scheme were used to estimate initial carbon pools and calibrate the model, since the C of POM (particle sizes >50 μm) has been associated with the RPM and DPM pool of RothC (Galdo et al., 2003; Krull et al., 2005; Gottschalk et al., 2010). Initial SOC was partitioned among the different carbon pools (RPM, DPM, BIO, IOM and HUM) using the following approach. The POM content is the sum of RPM and DPM fractions apportioned by calibration. Following RothC-26.3-model recommendations, BIO was assumed to be 3% of the total SOC and IOM using the equation suggested by Falloon et al. (1998): $IOM = 0.049SOC^{1.139}$. For the estimation of IOM content, we used the set-aside SOC content since the inert carbon it is not usually considered to change significantly because of cultivation in a few decades. However, due to the uncertainty of this assumption in the uncertainty analysis the range of the IOM pool is from zero to the value taken by the Falloon’s equation. Finally, the HUM pool was calculated by difference of the rest pools from the total SOC.

The developed excel version of the RothC model was used in combination with @RISK (PALISADES Corp.) in order to simulate the uncertainty in carbon turnover during set-aside conditions due to initial conditions and model parameters and inputs. First, RothC/@RISK was used in a Monte-Carlo fashion in order to identify the optimal/unique solution of model parameters and input that best simulates each soil. Plant litter input and six model parameters were considered simultaneously with uniform distributions (Table 4). Since the plant litter had not been measured, the appropriate range found in the literature for the specific climate and land use was used to constrain the model. The carbon input of plant residues for the set-aside field in Iowa (grassland) was the sum of average values for the above and below-ground (0-15 cm) potential input for recently restored grasslands in south central Iowa as 5 to 10 t C ha^{-1} (Guzman et al., 2010); while within this range has been also found the maximum litter residue (7.59 t C ha^{-1}) in prairies in central Missouri (Buyanovsky et al., 1987). Beier et al (2009) found in six shrublands across Europe that plant litter ranged from 1.0 to 5.3 t C ha^{-1} for the 0-20 cm soil depth and above ground litter contributed 14.7 to 62.3% (0.33 to 1.43 t C ha^{-1}). If we assume that 80% of the belowground litter was found in the 0-10 cm, which was the main rooting depth in all six sites as it is indicated in the study, the plant litter should range from 1 to 4.5 t C ha^{-1}. Similar values for litterfall in Mediterranean shrublands (0.65-1.45 t C ha^{-1}, assuming that carbon content of litterfall biomass is 50%, as it is indicated by the study) were reported by Fioretto et al (2003). An expanded range based on the values that have been reported in the literature was introduced for the RPM (0.1 to 0.8 y^{-1}) and HUM (0.0001 to 0.3 y^{-1}) decomposition rate constants. For the remaining model parameters (DPM and BIO decomposition rate constants, DPM-to-RPM ratio, and BIO%, the range was established as ±10% of their default RothC values.

Monte-Carlo simulations with 5000 iterations were conducted using the distributions of the plant input and the six model parameters described above. The solution with the lowest deviation (<±1%) from both SOC and POM measurements was considered as the optimum solution and the values of the parameters that generated the solution as the calibrated values. The assemble of solutions falling within the ±5% of the SOC and POM field measured values was also examined in order to confirm the uniqueness of the optimum solution. This assumption correspond to 5% standard uncertainty of the mean SOC and POM field measured value and stand for ±11% standard deviation of the SOC and POM field measured values, if it is assumed that five samples were taken and measured separately. The expanded range of plant input as well RPM and HUM decomposition rate constants was narrowed (Table 4), so as more iterations to pass the criterion and calculate better statistics. In particular, the standard deviations of the selected solutions of the plant input and the six model parameters were calculated and their values were compared with the initial distributions. Low standard deviations suggest the uniqueness of the optimum solution since the system is inherently constrained and does not allow solutions with extreme combinations of parameter values.

Once the model was calibrated, sensitivity analysis was conducted for the six model parameters (DPM, RPM, BIO, and HUM decomposition rate constants, DPM-to-RPM ratio, HUM%) and the plant litter input using ranges of ±10% and ±50% of the calibrated values.

Finally, the propagation of uncertainty in the simulated results due to initial conditions (SOC, DPM, RPM, BIO, HUM, and IOM carbon pools), plant litter input and soil clay content, as well the six model parameters used for calibration was conducted for each category separately and all together. The distribution for each parameter derived from the Monte-Carlo simulation for the iterations falling within the ±5% of the SOC and POM field measured values was used in the uncertainty analysis. Field variability for initial conditions and clay content could not be estimated since soil samples were only one composite of five subsamples. To overcome this issue, the distribution was selected to be normal having as mean the calibrated value and a standard deviation of 5% of the mean. The uncertainty of the IOM pool was considered to be a uniform distribution ranging from zero to the value obtained by Falloon’s equation. The HUM pool was calculated by difference.

3. Results and Discussion

3.1. Soil Characterization

The basic physicochemical soil measurements are presented in table 1. The pH of the set-aside IA soil was almost neutral (6.9), while the cropland soil pH was acidic due to fertilization (6.2). The pH of both Greek soils was basic (7.7-7.8) reflecting the calcaric composition of the soils. The macro-element abundances (K, Ca, Mg, Na) were generally increased, under set-aside conditions and this was also depicted in the increase of the soluble salts and the cation exchange capacity (CEC). Potential mineralizable N, potential soluble organic N and C, as well carbohydrate C increased in the set-aside soils by a factor of 4.9, 3.5, 2.9, and 2.7 for Iowa and only 1-1.5 times for Greece.

Set-aside from crop production in Iowa and Greek soils for 20 and 35 years, respectively, as it was indicated by the field measurements resulted in similar rates of C increase (0.777 and 0.648 t C ha^{-1} y^{-1}) in topsoil (10 cm), while the N increase was doubled for Iowa as compared with Greece (0.048 and 0.019 t N ha^{-1} y^{-1}). The measured increase of SOM was accompanied by 19 and 6 % decrease of soil bulk density for IA and GR, respectively. Subsoil carbon density in set aside and cropland fields in the Iowa site (Table 1) was found to differ only by about 2%, verifying our assumption that most of the SOM gain found in the topsoil where the dense root system is found (Potter and Derner, 2006). Therefore, accounting also for the subsoil (0-30 cm) the increase for the Iowa soil was found to be similar for C (0.736 t C ha^{-1} y^{-1}; 0-30 cm), being however double for nitrogen (0.088 t N ha^{-1} y^{-1}; 0-30 cm). The rates were similar with values for arable to grasslands conversions reported for French sites (0.48±0.26 t C ha^{-1} y^{-1}) (Soussana et al., 2004) as well sites in UK (0.3 to 0.8 t C ha^{-1} y^{-1}) (Ostle et al., 2009). The C-to-N ratio was lower in croplands compared to set-aside fields, likely indicating less stabilized SOM. The C-to-N ratios of the SOM increase in set-aside fields was found to be higher in Greece compared to Iowa, indicating the effect of the plant litter material quality (shrubland in Greece versus grassland in Iowa) and possibly less decomposed SOM.

Table 2 presents the (sand-free) WSA distribution of the four soils. The total WSA were found to be higher in set-aside fields by 68 % (IA) and 10 % (GR) compared to croplands. The increase of WSA weight and stability in set-aside soils was primarily attributed to large and medium sized macro-aggregate. The shift in composition to larger aggregates was very significant in the Iowa set-aside soil, were macro-aggregates increased by 110% comprising 82% of soil composition compared to cropland where they were 39%. In Greece, the increase was smaller (46%) and macro-aggregates comprised 66% in the set-aside soil. At the same time, decline was observed in the micro-aggregate and the silt-clay sized fractions. The shift in composition to larger aggregates caused an increase in the MWD by 108% (IA) and 52.5% (GR) in Iowa and Greece, respectively (Table 2).

Table 2 also presents the C and N content in the various aggregate fractions. Soil C in IA cropland was 16.8 g kg^{-1} with 60% in macro-aggregate fraction, while in IA set-aside was 35.5 g kg^{-1} with 90% in macro-aggregate fraction. Similarly, soil C in GR cropland was 29.1 g/kg with 58% in macro-aggregate fraction, while in GR set-aside was 52.2 g kg^{-1} with 71% in macro-aggregate fraction. Similar patterns were also observed for N.

The C and N concentration increased up to 2 times in the aggregate fractions in the Greek set-aside soil compared to cropland (Fig. 1). The C content of the easily dispersed silt-clay sized fraction (sc-M), the micro-aggregate related silt-clay fraction (sc-mM) and the free silt-clay sized aggregates in the Greek set-aside soil were found to be significantly higher compared to the respective concentrations of cropland, while the N content was similar. The increase of C and N concentration in macro-aggregates was attributed both to POM and mineral fractions. The POM contribution in the composite macro-aggregate fraction was 44 and 51% in set-aside and cropland field and 38 and 34 % in the 250-1000 μm fraction.

In Iowa set-aside soil increase of C and N concentration was observed only in macro-aggregates while in finer aggregates presented lower concentration (Fig. 1). The latter has been also observed by Emadi et al (2009). The micro-aggregate isolation confirmed that all the mineral fractions in Iowa set aside field exhibited lower concentrations compared to the cropland. Don et al., 2009 also found that the conversion of cropland into grassland in a soil with very low clay content (5-7%) in contrast with a rich in clay soil (30%) did not resulted in the increase of the mineral-associated carbon fraction as it was limited by total clay surface area available for carbon stabilization. The increase of C and N concentration in macro-aggregates was attributed to POM. The C content of the composite and the 250-1000 μm aggregate fraction attributed to POM in the Iowa cropland was 19% and 23%, respectively and changed to 63% and 50% in the set-aside field.

The C-to-N ratio increased in aggregate fractions of set aside soils, indicating less decomposed SOM as compared to croplands. The relative increase was found to be higher in Greece compared to Iowa, indicating the effect of the plant material (shrubs) and possibly less decomposed SOM. More labile SOM indicated by higher C-to-N ratio (Elliot, 1986) was found in macro-aggregates, attributed to the increase of C-to-N ratio of the POM fractions in Iowa and both POM and mineral fractions in Greece.

As the size and stability of water stable aggregates decreases, their turnover rate has been found to increase (Six et al., 2000). The ratio of the fPOM-C to cPOM-C has been suggested (Six et al., 2000) as an indication of turnover rate (the higher the ratio, the lower the turnover rate). The fPOM-C to cPOM-C ratio of the composite macro-aggregates (IA: 7.9, GR: 6.4) and the small macro-aggregates (IA: 9.5, GR: 7.5) in cropland soils is lower as compared with set aside fields (composite macro-aggregates IA: 10, GR: 13.2 and small macro-aggregates IA: 23.4, GR: 10.2). Therefore the turnover rate is higher in croplands due to tillage and plant litter input quality. In addition, the estimated turnover rates in Iowa are significantly lower for the small macro-aggregates compared with the composite macro-aggregates suggesting in accordance with the lower C-to-N ratio in the 250-1000 μm fraction more decomposed and older POM. On the contrary, this pattern was not observed in Greece, where C-to-N ratio was high even in micro-aggregates, indicating possible lower decomposition rates.

3.2. Carbon turnover modeling

The clay content for the IA soil was 7% (Table 1), the initial SOC 18.6 t C ha^{-1} and the initial POM 2.6 t C ha^{-1} (Table 3). The initial carbon apportioning for the Iowa soil procedure was 1.94 t C ha^{-1} for RPM, 0.68 t C ha^{-1} for DPM, 0.56 t C ha^{-1} for BIO, and 2.63 t C ha^{-1} for IOM. By difference the initial HUM pool was 12.78 t C ha^{-1}. The simulation results were compared with the results presented in Table 3 for the set-aside field (SOM = 33 t C ha^{-1}, POM = 20 t C ha^{-1}). The clay content for the GR soil was 30% (Table 1), the initial SOC 34.3 t C ha^{-1} and the initial POM 14.3 t C ha^{-1} (Table 3). The initial carbon apportioning for the Greek soil procedure was 14 t C ha^{-1} for RPM, 0.3 t C ha^{-1} for DPM, 1.03 t C ha^{-1} for BIO, and 5.05 t C ha^{-1} for IOM. By difference the initial HUM pool was 13.89 t C ha^{-1}. The simulation results were compared with the results presented in Table 3 for the set-aside field (SOM = 58.5 t C ha^{-1}, POM = 21.8 t C ha^{-1}).Table 4 presents the Monte-Carlo simulation results where the plant litter input and model parameters were allowed to vary. The optimum solution was used in order to obtain the calibrated model results (Table 4). The calibrated values for Iowa were 5.05 t C ha^{-1} for plant litter input and 0.34 y^{-1} for RPM and 0.27 y^{-1} for HUM, while for Greece were 3.79 t C ha^{-1} for plant litter input and 0.21 y^{-1} for RPM and 0.0041 y^{-1} for HUM.

The statistics of the assemble of simulations that fall within ±5% of both SOC and POM measurements are also presented in Table 4. The distribution type in most of the parameters was found to be triangle and some of them uniform and beta general. The standard variation was found to be less than 10% of the mean value for all parameters apart from the RPM decomposition rate constant where it was 13.9%, in the case of Iowa. Similarly, in Greece, the standard variation was found to be less than 10% of the mean value for all parameters while for the RPM and HUM decomposition rate constants was 10.6% and 58.1%, respectively. The narrow values of the resulted standard deviations confirm the uniqueness of optimum solution since they represent a well constrained system that does not allow acceptable solutions with extreme parameter value combinations.

For Iowa, the 'adjusted' model was able to capture the increase of POM and SOC content very well, which was likely attributed to POM material. Monthly decomposition rates for RPM and HUM pools for both sites are presented in Table S2 in the supporting information material. The annual decomposition rate for RPM was found to be 0.093 y^{-1} and 0.105 y^{-1} for Iowa and Greece, respectively, while for HUM was 0.075 y^{-1} and 0.002 y^{-1}, likewise. The high decay constant of the HUM pool in Iowa could be attributed to the very low clay content in accordance with Balesdent et al. (1998) and Gottschalk et al. (2010). Balesdent et al. (1998) showed that SOC in the size fraction <50 μm is made up of the relatively rapidly decomposing pool of silt associated C, and a relatively slowly decomposing pool of clay associated C. The measured clay turnover associated C had a decay constant of 0.03 y^{-1} (Balesdent et al., 1998), while the silt associated C had a measured decay constant of 0.12 y^{-1}, declining almost as rapidly as that in the POM fraction, especially under cultivation (Gottschalk et al., 2010). Nevertheless, the wet and warm summers in Iowa stimulated organic matter decomposition.

Similarly, in Greece, the 'adjusted' model was able to capture the increase of POM, HUM and SOC content, and the results were consistent with the fractionation measurements where the increase in carbon stock was attributed to both POM and HUM material. Lower HUM decomposition rate in Greece is attributed to dry climatic conditions and high clay content which result in higher protection. Slaking of the soil surface can result in fine soil particles moving into inter-aggregate pores in the surface area, which can reduce the infiltration rate of rainfall or irrigation water and reduce hydraulic conductivity (Hillel, 1998). In addition, residue quality (lignin/N ratio, C/N ratio and N concentration) of shrublands affects the rate of decomposition and the aggregation rate (Aerts, 1997; Sainju et al., 2003).

Sensitivity analysis at the ±10% and ±50% ranges of the calibrated values for the six model parameters and the plant input was conducted. The tornado graphs are presented in Figure 2 and the sensitivity coefficients (the absolute value of the ratio: $(\Delta Y/Y)/(\Delta x/x)$) in Table S3 in the supporting information material. In both sites the total plant litter input and the RPM decomposition rate constant had the highest sensitivity. In Iowa, the BIO% as well as the BIO and DPM decomposition rate constants presented the lowest sensitivity with coefficients lower than 0.1 and 0.07 for the 50% and 10% case, respectively. In Greece, the coefficients were found to be in general lower than 0.04 for HUM, BIO and DPM decomposition rate constants for both the 50% and 10%. The results emphasize the importance of measurement of plant litter input when conducting carbon sequestration studies as well as the necessity of developing a methodology to model carbon sequestration in soils in the absence of such measurements.

A comparison of the optimum simulation for both SOC and POM and the uncertainties attributed to the initial conditions (SOC, DPM, RPM, BIO, HUM, and IOM carbon pools) the input data (plant litter input and clay content), and the six model parameters used for calibration parameters (DPM, RPM, BIO, and HUM decomposition rate constants, DPM-to-RPM ratio, HUM%), in terms of the mean of the assemble of Monte Carlo simulations plus one standard deviation are presented in Figure 3. In addition, Figure S3 presents the distribution of cumulative accumulation of total carbon after 100 years of set aside conditions due to uncertainties in initial condition, input and parameter values as well as the expected accumulation from the optimum simulation. In Iowa, the uncertainty of prediction (90% of the distribution, range between 5 and 95%) due to input data, model parameters, and initial conditions corresponded to 43.3%, 51%, and 14.3% of the total carbon sequestrated in the 100 years, respectively and the probability of over predicting carbon sequestration was at the same order 0.94, 0.25, and 0, respectively. Similarly, the uncertainty of POM due to input data, model parameters, and initial conditions corresponded to 25.5%, 42.4%, and 0% of the total increase in POM in the 100 years, respectively and the probability of over predicting POM was 0.94, 0.21, and 1, respectively. In Greece, the uncertainty of prediction due to input data, model parameters, and initial conditions corresponded to 42.1%, 49.5%, and 13% of the total carbon sequestrated in the 100 years, respectively and the probability of over predicting carbon was 0.69, 0.24, and 0.12, respectively. Similarly, the uncertainty of POM due to input data, model parameters, and initial conditions corresponded to 90.5%, 102%, and 0% of the total increase in POM in the 100 years, respectively and the probability of over predicting POM was 0.7, 0.29, and 0. The Iowa soil was projected to sequester 17.5 t C ha^{-1} and the Greek soil 54 t C ha^{-1} in 100 years. Overall, the uncertainty of the model predictions for SOC and POM (65.6% and 140% of the total carbon sequestrated and POM increase for Iowa and 70.8% and 51.6% of the total SOC and POM increase for Greece, respectively) were quite significant, while the probability of over predicting SOC and POM (0.4 and 0.64 for Iowa and 0.31 and 0.46 for Greece) suggested that the mean of the Monte Carlo simulation distributions were close to the optimum simulation. Overall, our analysis showed that the resulting uncertainties are important; hampering our ability to accurately predict carbon sequestration under set aside conditions (even in the absence of climate change impacts). These results emphasize the necessity of obtaining accurate plant input data and other physical soil parameters as well as quantifying the variability of initial conditions in order to reduce the uncertainty of carbon sequestration projections.

4. Conclusions

A Monte Carlo based methodology was developed to assess the uniqueness of solution carbon sequestration modeling of cultivated to set aside conditions and the uncertainties due to initial conditions, model parameters and time series of the RothC carbon model.

- POM-carbon data obtained by soil physical fractionation were used successfully to initialize and calibrate the carbon model and provided boundary conditions to effectively constrain the solution of the model.
- The calibrated RPM decomposition rate constants in Iowa, similarly with the HUM decomposition rate constants, was higher (13.3 %) and in Greece lower (31%) than the defaults rates suggesting that commonly used RothC model functions for decomposition rate correction due to temperature systematically underestimate decomposition at low temperatures and overestimate decomposition at high temperatures.
- The calibrated HUM decomposition rate constants were significantly different than the defaults rates in both Iowa (13.5 times higher) and Greece (48.8 times lower). The significant difference between the two sites is attributed to significant differences in clay content. Finer texture in Greece resulted in higher protection of the HUM pool and presumably lower ‘apparent’ sensitivities (Davidson and Janssens, 2006, Kleber and Johnson, 2010) to temperature and/or moisture effect on decomposition in contrast with the coarser Iowa site where the opposite pattern was observed.
- Model sensitivity analysis revealed that total plant litter input and the RPM decomposition rate constant exhibited the highest sensitivity on predicted SOC in both sites.

- Uncertainty analysis suggested that total uncertainty of carbon sequestration under set aside from crop production conditions over 100 years can be as much as 70% of the total amount that was sequestrated in both the Greek and Iowa soil. In both sites plant litter input was a major source of uncertainty. The uncertainty analysis results underlie the importance of obtaining accurate plant input data for set aside land uses for the various climates in the world in order to minimize carbon sequestration estimates and determine more accurate the variability of carbon transformation rate constants as a function of climatic conditions.

The methodology developed in this study can be used to assess the factors affecting carbon sequestration in agricultural soils, quantify the uncertainties in predictions as well as assist in the design of field experiments and measurements to minimize the uncertainties and improve carbon sequestration estimates that relate directly to soil fertility.

Acknowledgement

We would like to acknowledge the financial support by the University of Iowa IIHR Hydroscience and Engineering Institute, the Technical University of Crete-Research Committee, the FP6 Project SoilCritZone and the FP7 Project SoilTrec. We would like also to acknowledge Gorana Rampazzo Todorovic for providing us with an initial excel version of the RothC model. F.E. Stamati was supported by a Ph.D. fellowship from Bodosaki Foundation. The authors are grateful of Prof. Thanos Papanikolaou and Aaron Gwinnup for field assistance in Iowa sampling.

Supplementary Information

Additional supporting information may be found in the online version of this article. Methods on physical fractionation and soil physicochemical analysis, soil organic carbon content in topsoil and subsoil in Koiliaris River Basin (Fig. S1), physical fractionation scheme used in the study (Fig. S2), the output distributions by the Monte-Carlo simulations for the calculation of uncertainties. (Fig. S3), meteorological data used for the application of the RothC model (Table S1), monthly and annual decomposition rates for RPM and HUM pools (Table S2), and sensitivity coefficients for RothC model parameters (Table S3).

References

Aerts, R., 1997. Climate, Leaf Litter Chemistry and Leaf Litter Decomposition in Terrestrial Ecosystems: A Triangular Relationship. Oikos 79, 439-449.

Angers D.A., Carter, M.R., 1996. Aggregation and organic matter storage in cool, humid agricultural soils. In: Carter M.R., Stewart B.A., eds. Structure and organic matter storage in agricultural soils. Boca Raton, FL: Lewis Publ, 193-211.

Balesdent, J., Besnard, E., Arrouays D., Chenu, C., 1998. The dynamics of carbon in particle-size fractions of soil in a forest-cultivation sequence. Plant and Soil 201, 49–57.

Banwart, S., Bernasconi, S.M., Bloem, J., Blum, W., Brandao, M., Brantley, S., Chabaux, F., Duffy, C., Kram, P., Lair, G., Lundin, L., Nikolaidis, N., Novak, M., Panagos, P., Ragnarsdottir, K.V., Reynolds, B., Rousseva, S., de Ruiter, P., van Gaans, P., van Riemsdijk, W., White, T., Zhang, B., 2011. Assessing Soil Processes and Function in Critical Zone Observatories: hypotheses and experimental design. Vadose Zone Journal 10, 974-987.

Batlle-Aguilar, J., Brovelli, A., Porporato, A., Barry, D.A., 2010. Modelling soil carbon and nitrogen cycles during land use change: a review. Agronomy for Sustainable Development 31, 251-274.

Beier, C., Emmett, B.A., Tietema, A., Schmidt, I.K., Penuelas, J., Lang, E.K., Duce, P., De Angelis, P., Gorissen, A., Estiarte, M., de Dato, G.D., Sowerby, A., Kröel-Dulay, G., Lellei-Kovács, E., Kull, O., Mand, P., Petersen, H., Gjelstrup, P., Spano, D., 2009. Carbon and nitrogen balances for six shrublands across Europe. Global Biogeochemical Cycles, 23 (GB4008), p. 13. ISSN 0886–6236.

Bouyoucos, G.J., 1936. Directions for making mechanical analysis of soils by the hydrometer method. Soil Science 4, 225-228.

Buyanovsky, G.A., Kucera, C.L., Wanger, G.H., 1987. Comparative analyses of carbon dymanics in native and cultivated ecosystems. Ecology 68, 2023-2031.

Coleman, K., Jenkinson, D.S., 1999. RothC-26.3 - A Model for the turnover of carbon in soil: Model description and windows users guide: November 1999 issue. Lawes Agricultural Trust Harpenden. ISBN 0 951 4456 8 5

David, M.B., McIsaac, G.F., Darmody, R.G., Omonode, R.A., 2009. Long-Term Changes in Mollisol Organic Carbon and Nitrogen. Journal of Environmental Quality, 38, 200–211.

Davidson, E.A., Janssens, I.A. 2006. Temperature sensitivity of soil carbon decomposition and feedbacks to climate change. Nature 440, 165–173.

Don, A., Scholten, T., Schulze E.D., 2009. Conversion of cropland into grassland: Implications for soil organic-carbon stocks in two soils with different texture. Journal of Plant Nutrition and Soil Science 172, 53–62

Elliott, E.T., 1986. Aggregate structure and carbon, nitrogen, and phosphorus in native and cultivated soils. Soil Science Society of America Journal 50, 627-633.

Emadi, M., Baghernejad, M., Memarian, H.R., 2009. Effect of land-use change on soil fertility characteristics within water-stable aggregates of two cultivated soils in northern Iran. Land Use Policy 26, 452–457.

Falloon, P.D., Smith, P., 2000. Modelling refractory soil organic matter. Biology and Fertility of Soils 30, 388-398.

Falloon, P., Smith, P., Coleman, K., Marshall, S., 1998. Estimating the size of the inert organic matter pool from total soil organic carbon content for use in the Rothamsted Carbon model. Soil Biology and Biochemistry 30, 1207–1211.

FAO 1998. Wold Reference Base for Soil Resources. (http://www.fao.org/ag/agl/agll/wrb/)

Fioretto, A., Papa, S., Fuggi, A. 2003. Litter-fall and litter decomposition in a low Mediterranean shrubland. Biology and Fertility of Soils 39, 37–44

Galdo, I.D., Six, J., Peressotti, A., Cotrufo, M.F., 2003. Assessing the impact of land-use change on soil C sequestration in agricultural soils by means of organic matter fractionation and stable C isotopes. Global Change Biology 9, 1204–1213.

Gottschalk, P., Bellarby, J., Chenu, C., Foereid, B., Smith, P., Wattenbach, M., Zingore, S., Smith, J., 2010. Simulation of soil organic carbon response at forest cultivation sequences using 13C measurements. Organic Geochemistry 41, 41–54.

Guo, L.B., Gifford, R.M., 2002. Soil carbon stocks and land use change: a meta analysis. Global Change Biology 8, 345–360.

Guzman, J.G., Al-Kaisi, M.M., 2010. Soil Carbon Dynamics and Carbon Budget of Newly Reconstructed Tall-grass Prairies in South Central Iowa. Journal of Environmental Quality 39, 136–146.

Hillel, D. 1998. Environmental Soil Physics. Academic Press. San Diego, CA

Juston, J., Andrén, O., Kätterer, T., Jansson, P.E., 2010. Uncertainty analyses for calibrating a soil carbon balance model to agricultural field trial data in Sweden and Kenya. Ecological Modeling 221, 1880-1888.

Kleber, M., Johnson, K.J., 2010. Advances in Understanding the Molecular Structure of Soil Organic Matter: Implications for Interactions in the Environment. Advances in Agronomy 106, 77-142.

Krull, E.S., Skjemstad, J.O., Burrows, W.H., Bray, S.G., Wynn, J.G., Bol, R. et al. 2005. Recent vegetation changes in central Queensland, Australia: Evidence from δ13C and 14C analyses of soil organic matter. Geoderma 12, 241–259.

Lal R. 1997. Residue management, conservation tillage and soil restoration for mitigating greenhouse effect by CO2-enrichment. Soil and Tillage Research, 43, 81-107.

Lichter, K., Govaerts, B., Six, J., Sayre, K.D., Deckers, J., Dendooven, L., 2008. Aggregation and C and N contents of soil organic matter fractions in a permanent raised-bed planting system in the highlands of Central Mexico. Plant and Soil, 305, 237-252.

Manzoni, S., Porporato, A., 2009. Soil carbon and nitrogen mineralization: Theory and models across scales, Soil Biology and Biochemistry 41, 1355-1379.

Methods of Soil Analysis, Part 3- Chemical Methods, 2nd Ed. Rev. Soil Science Society of America, Black, C.A et al., 1982.

Nikolaidis, N.P., Bidoglio, G., 2011. Conceptual modeling of soil organic matter and structure dynamics: a synthesis. Geoderma (submitted revisions).

Ostle, N.J., Levy, P.E., Evans, C.D., Smith, P., 2009. UK land use and soil carbon sequestration-Review. Land Use Policy 26S, S274–S283.

Paul, K.I., Polglase, P.J., Richards, G.P., 2003. Predicted change in soil carbon following afforestation or reforestation, and analysis of controlling factors by linking a C accounting model (CAMFor) to models of forest growth (3PG), litter decomposition (GENDEC) and soil C turnover (RothC). Forest Ecology and Managment 177, 485-501.

Piccolo, A., Zena, A., Conte, P., 1996. A comparison of acid hydrolyses for the determination of carbohydrate content in soils. Communication in Soil Science and Plant analysis 27, 2909-2915.

Potter, K.N., Derner, J.D., 2006. Soil carbon pools in central Texas: Prairies, restored grasslands, and croplands. Journal of Soil and Water Conservation 61, 124-128.

Rees, R.M., Bingham, I.J., Baddeley, J.A., Watson, C.A., 2005. The role of plants and land management in sequestering soil carbon in temperate arable and grassland. Geoderma 128, 130-154.

Sainju, U.M., Whitehead, W.F., Singh. B.P., 2003. Cover crops and nitrogen fertilization effects on soil aggregation and carbon and nitrogen pools. Canadian Journal of Soil Science 83, 155–165.

Six, J., Elliott, E.T., Paustian, K., 2000. Soil macroaggregate turnover and microaggregate formation: a mechanism for carbon sequestration under no tillage agriculture. Short Communication in Soil Biology and Biochemistry 32, 2099-2103.

Shibu, M.E., Leffelaar, P.A., Van Keulen, H., Aggarwal, P.K., 2006. Quantitative description of soil organic matter dynamics – A review of approaches with reference to rice-based cropping systems. Geoderma, 137, 1-18.

Smith, P., Powlson, D.S., Smith, J.U., Elliott, E.T., 1997. Evaluation and comparison of soil organic matter models using datasets from seven long-term experiments. Geoderma 81, 1-225.

Soussana, J.F., Loiseau, P., Vuichard, N., Ceschia, E., Balesdent, J., Chevallier, T., Arrouays, D., 2004. Carbon cycling and sequestration opportunities in temperate grasslands. Soil Use and Management 20, 219-230.

The World Factbook, 2008 (https://www.cia.gov/library/publications/the-world-factbook/)

Todorovic, G.R., Stemmer, M., Tatzber, M., Katzlberger, C., Spiegel, H., Zehetner, F., Gerzabek, M.H., 2010. Soil-carbon turnover under different crop management: Evaluation of RothC-model predictions under Pannonian climate conditions. Journal of Plant Nutrition and Soil Science 173, 662–670.

Tufekcioglu, A., Raich, J.W., Isenhart, T.M., Schultz R.C., 2003. Biomass, carbon and nitrogen dynamics of multi-species riparian buffers within an agricultural watershed in Iowa, USA. Agrogorestry Systems 57, 187-198.

Wagai, R., Mayer, L.M., Kitayama, K., Knicker, H., 2008. Climate and parent material controls on organic matter storage in surface soils: three-pool, density-separation approach. Geoderma 147, 23-33.

Zimmermann, M., Leifeld, J., Schmidt, M.W.I., Smith, P., Fuhrer, J., 2007. Measured soil organic matter fractions can be related to pools in the RothC model. European Journal of Soil Science 58, 658–667.

List of Figure Captions

Fig. 1. a) C and b) N concentration of the sand free aggregate fractions (g kg^{-1}). Values are shown as means (n=3). Standard deviation was lower than 1-3% for OC and 1-4% for TKN. Mean values followed by the same lowercase letter under the same series label are not significantly different ($p<0.05$). Mean values followed by the same uppercase letter under the same x-axis legend are not significantly different ($p<0.05$).

Fig. 2. Tornado Graphs for 10% (black indicated) and 50% (grey indicated) sensitivity analysis. RPM=resistant plant material decomposition rate constant, DPM=decomposable plant material decomposition rate constant, HUM=humus decomposition rate constant, BIO= biomass decomposition rate constant, DPM/RPM ratio=the apportionment ratio of plant litter input DPM and RPM carbon pools, BIO%=The proportion that goes to BIO (100-BIO% is the proportion that goes to HUM).

Fig. 3. Uncertainty of total organic carbon (TOTAL) and particulate organic matter (POM) due to model parameters, input data, and initial conditions, as well as the total uncertainty, compared with the optimum solution (calibration).

Table 1. Chemical and physical properties of IA and GR soils.

	Iowa		Greece	
	Cropland	**Set-aside**	**Cropland**	**Set-aside**
Bulk Density /kg m^{-3}	1110/1217[a]	930/1024[a]	1180	1110
pH	6.2	6.9	7.8	7.7
Sand /%	38	63	30.1	27.4
Clay /%	7	7	30	30
OC[b] /% – BS[c]/AF[d]/Subsoil	1.70/1.68/1.59	3.70/3.55/1.85	2.94/2.90	5.17/5.27
N /% - BS/AF/Subsoil	0.14/0.14/0.11	0.27/0.26/0.17	0.24/0.22	0.32/0.31
C-to-N - BS/AF	11.7/11.7	13.6/13.8	12.3/12.9	16.4/16.9
Recovery /%-AF: OC/TKN	98.5/98.5	95.9/94.3	98.6/93.5	102/99.3
Soluble salts /mmhos cm^{-1}	0.11	0.17	0.36	0.61
CEC /meq $100g^{-1}$	6.8	11.5	24.1	36.3
P /mg kg^{-1}	113.1	106.1	343.9	56.5
K /mg kg^{-1}	141.4	614.7	702.9	290.8
Ca /mg kg^{-1}	2694.1	5548.8	9947.1	16087.7
Mg /mg kg^{-1}	133.3	474.9	571.8	1046.1
S /mg kg^{-1}	20.2	21.7	60.8	125.2
B /mg kg^{-1}	1.4	2.2	5.5	7.9
Cu /mg kg^{-1}	2.8	4.1	15.6	11.3
Fe /mg kg^{-1}	462.5	327.8	165.3	305.0
Mn /mg kg^{-1}	26.3	248.3	258.4	133.3
Zn /mg kg^{-1}	4.4	11.6	11.2	5.9
Na /mg kg^{-1}	34.3	53.0	76.0	234.3
Bicarb-P /mg kg^{-1}	42.4	69.9	106.4	62.6
PMN /mg kg^{-1}	15.8	78.3	31.2	43.9
PSON /mg kg^{-1}	21.4	74.4	23.5	36.0
PSOC /mg kg^{-1}	132.7	390.7	228.9	360.8
Carbohydrate-C /mg kg^{-1}	45.1	123.1	42.0	42.3

[a] For the 10-30 cm subsoil.
[b]The Set-aside and cropland GR exhibited 0.98 and 0.17 % inorganic carbon content, respectively, while the rest lower than 0.03 %.
[c]BS: Bulk Soil.
[d]AF: Aggregate Fractionation.

Table 2. Soil water stable aggregate distribution (WSA, g sand-free aggregate100 g^{-1} soil), particle recovery, and mean weight diameter (MWD) as well C and N distribution among aggregates fractions (g kg^{-1}). Values are shown as means and standard deviation is given in the brackets (n=3). Mean values followed by the same lowercase letter within the same column are not significantly different (*p*<0.05). Mean values followed by the same uppercase letter within the same row are not significantly different (*p*<0.05).

	Cropland IA			**Set-aside IA**			**Cropland GR**			**Set-aside GR**		
	WSA	**C**	**N**	**WSA**	**C**	**N**	**WSA**	**C**	**N**	**WSA**	**C**	**N**
> 2000 μm	8.2 (4.8)b, C	1.5	0.11	34.6 (3.3)a, A	12.8	0.96	16.6 (1.1)b, B	6.0	0.46	29.6 (5.8)a, A	16.1	1.03
1000-2000 μm	0.4 (0.04)c, D	0.2	0.01	15.7 (2.5)b, A	6.5	0.47	2.9 (0.5)d, C	1.4	0.09	8.1 (1.6)c, B	4.5	0.27
250-1000 μm	30.2 (4.4)a, AB	8.3	0.77	31.4 (2.4)a, A	12.7	0.87	26.5 (1.8)a, B	9.3	0.67	27.9 (2.4)a, AB	16.8	1.00
53-250 μm	9.4 (2.4)b, C	5.1	0.41	5.9 (0.4)c, C	3.0	0.22	23.7 (0.6)a, A	9.5	0.78	15.9 (2.8)b, B	12.6	0.65
< 53 μm	5.3 (1.1)b, B	1.7	0.13	2.2 (0.3)d, C	0.5	0.04	10.1 (0.7)c, A	2.9	0.24	5.6 (0.7)c, B	2.8	0.17
Recovery (%)	94.5 (1.0)			93.1 (1.6)			91.5 (1.5)			94.6 (3.6)		
WSA	53.4 (1.8) B			89.8 (0.19) A			79.6 (0.4) C			87.2 (2.0) A		
WSA (>250 μm)	38.7 (4.0) B			81.7 (0.10) A			45.8 (1.5) D			65.5 (5.3) C		
MWD (mm)	1.16 (0.51) B			2.42 (0.24) A			1.36 (0.09) B			2.07 (0.38) A		

Table 3. Distribution of C and N in the particulate organic matter (POM) and in the silt-clay fractions (t C ha^{-1}).

	Total	**POM-fractions**	**Silt-clay fractions**
C			
Cropland IA	18.6	2.6	16.0
Set-aside IA	33.0	20.0	13.0
Cropland GR	34.3	14.3	20.6
Set-aside GR	58.5	21.8	36.8
N			
Cropland IA	1.6	0.2	1.3
Set-aside IA	2.4	1.2	1.2
Cropland IA	2.6	0.8	1.9
Set-aside IA	3.5	1.7	1.8

Table 4. Parameter information about the input and output distributions for the Monte-Carlo simulation and the optimum solutions.

Parameter	**total plant input**	**DPM/RPM ratio**	**BIO%**	**DPM**	**RPM**	**BIO**	**HUM**
RothC default values	input	1.44 (grassland) 0.67 (shubland)	46	10	0.3	0.66	0.02
IOWA							
Input of MonteCarlo simulation							
distribution type	Uniform	Uniform	Uniform	Uniform	Uniform	Uniform	Uniform
min	5.00	1.30	41.40	9.00	0.30	0.59	0.10
max	10.00	1.58	50.60	11.00	0.80	0.73	0.30
Statistics for the iterations passed the criterion[a]							
distribution type	Triang	BetaGeneral	Triang	Triang	Triang	Triang	Triang
min	5.01	1.32	41.47	8.66	0.32	0.59	0.22
max	6.47	1.58	49.84	10.99	0.56	0.72	0.30
mean	5.50	1.44	47.05	10.21	0.40	0.68	0.27
std	0.35	0.09	1.97	0.55	0.06	0.03	0.02
Chi-sq	0.43	6.24	2.43	0.90	1.29	1.29	2.43
Optimum solution (<0.70%)	5.05	1.51	48.90	10.37	0.34	0.69	0.27
GREECE							
Input of MonteCarlo simulation							
distribution type	Uniform	Uniform	Uniform	Uniform	Uniform	Uniform	Uniform
min	2.00	0.60	41.40	9.00	0.10	0.59	0.0001
max	4.50	0.74	50.60	11.00	0.30	0.73	0.04
Statistics for the iterations passed the criterion[a]							
distribution type	Triang	BetaGeneral	Triang	Uniform	BetaGeneral	Uniform	Triang
min	2.95	0.60	41.41	8.99	0.14	0.59	0.00
max	4.49	0.73	50.64	10.97	0.26	0.72	0.02
mean	3.98	0.67	46.03	9.98	0.22	0.66	0.01
std	0.36	0.04	2.66	0.57	0.02	0.04	0.01
Chi-sq	7.44	9.26	10.69	3.36	3.81	6.76	2.00
Optimum solution (<0.30%)	3.79	0.67	44.95	10.45	0.21	0.60	0.0041

[a]Statistics for the iterations passed the criterion of SOC and POM falling within the ±5% of the field measured values.

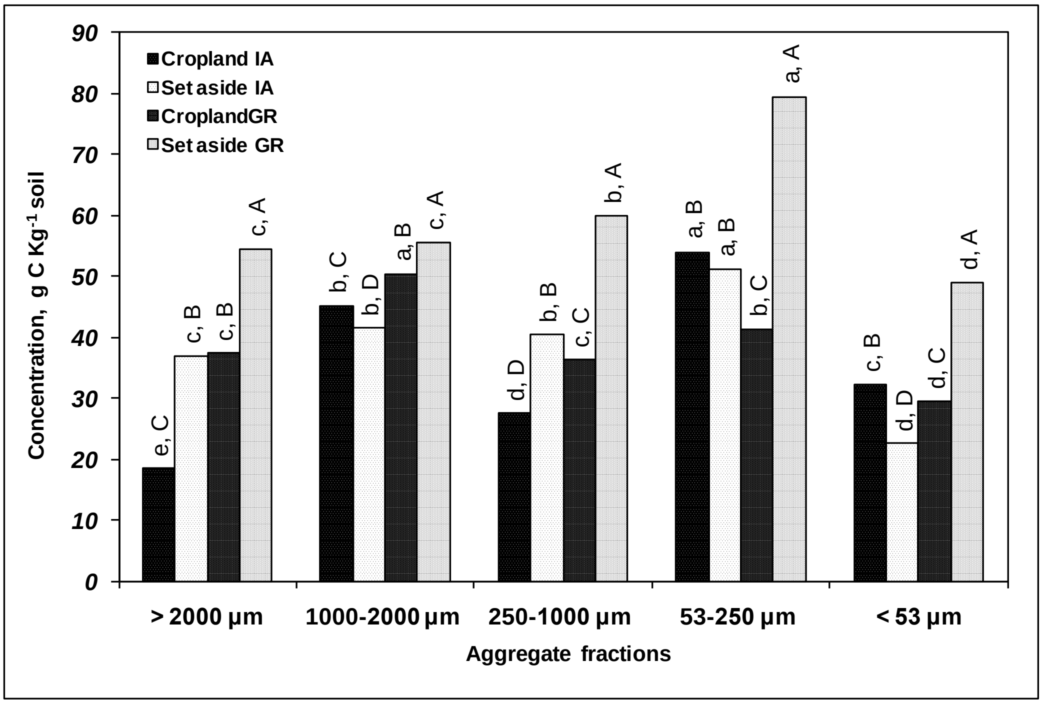
Cropland IA
Set aside IA
CroplandGR
Set aside GR
Concentration, g C Kg-1 soil
> 2000 µm
1000-2000 µm
250-1000 µm
53-250 µm
< 53 µm
Aggregate fractions

(a)

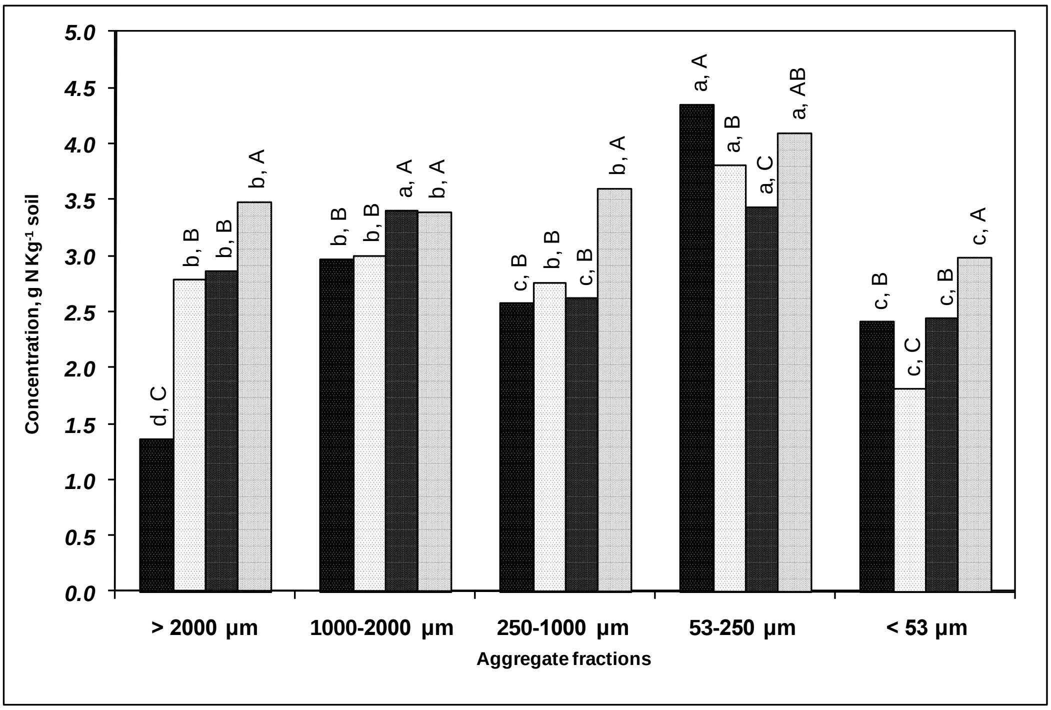
Concentration, g N Kg-1 soil
> 2000 µm
1000-2000 µm
250-1000 µm
53-250 µm
< 53 µm
Aggregate fractions

(b)

Fig. 1.

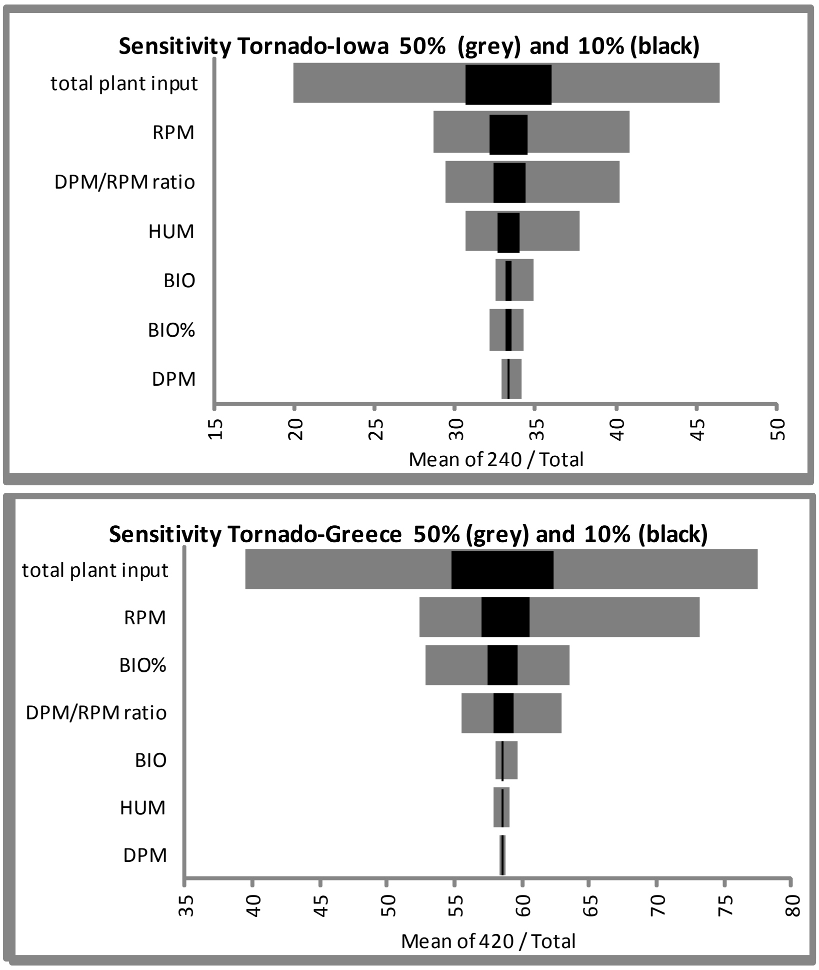
Sensitivity Tornado-Iowa 50% (grey) and 10% (black)
total plant input
RPM
DPM/RPM ratio
HUM
BIO
BIO%
DPM
15
20
25
30
35
40
45
50
Mean of 240 / Total
Sensitivity Tornado-Greece 50% (grey) and 10% (black)
total plant input
RPM
BIO%
DPM/RPM ratio
BIO
HUM
DPM
35
40
45
50
55
60
65
70
75
80
Mean of 420 / Total

Fig. 2.

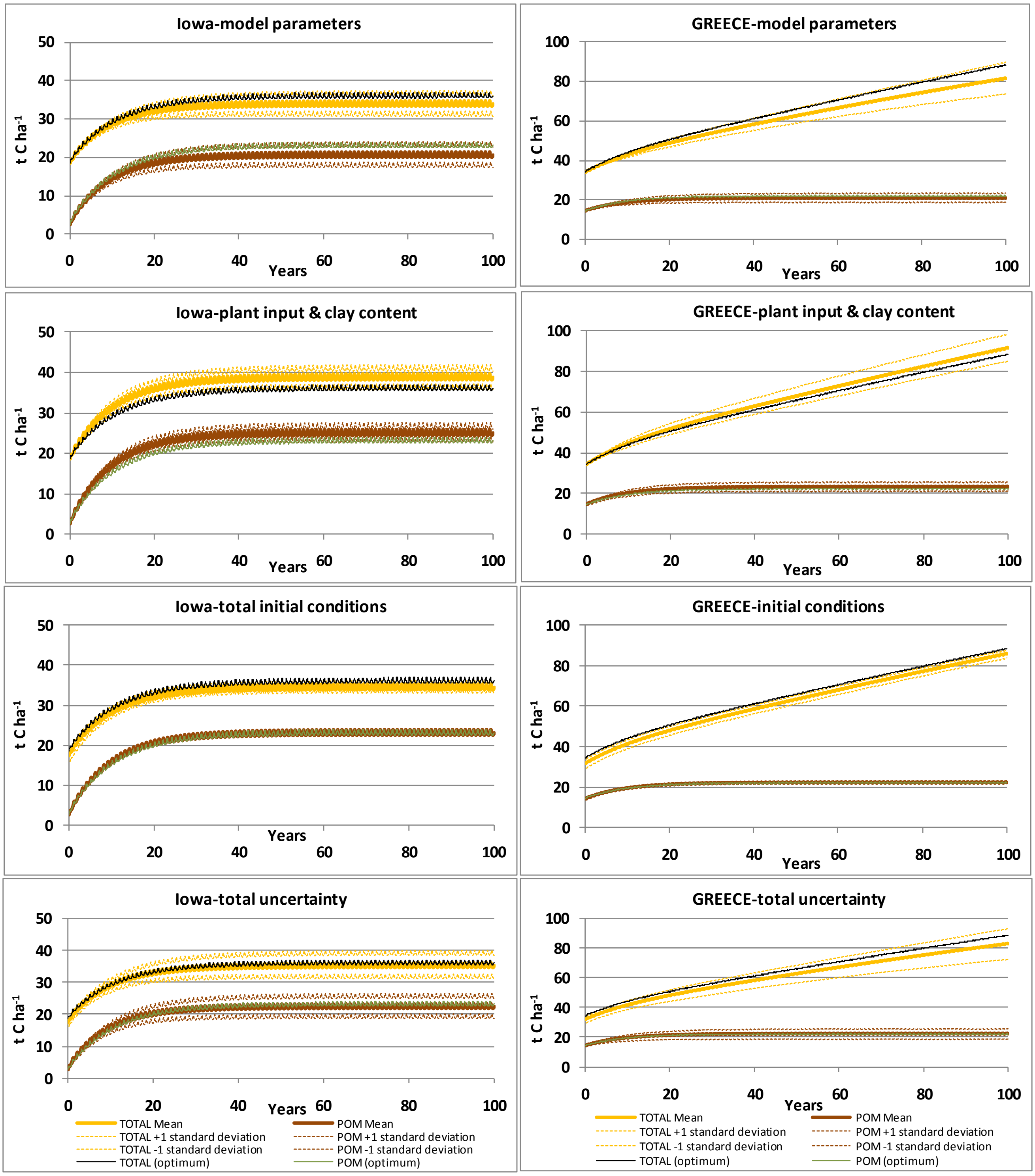
Iowa-model parameters
GREECE-model parameters
Iowa-plant input & clay content
GREECE-plant input & clay content
Iowa-total initial conditions
GREECE-initial conditions
Iowa-total uncertainty
GREECE-total uncertainty
t C ha-1
Years
TOTAL Mean
TOTAL +1 standard deviation
TOTAL -1 standard deviation
TOTAL (optimum)
POM Mean
POM +1 standard deviation
POM -1 standard deviation
POM (optimum)

Fig. 3.

SUPPLEMENTARY INFORMATION

Fotini E. Stamati, Nikolaos P. Nikolaidis, Jerald P. Schnoor

Modeling topsoil carbon sequestration in two contrasting crop production to set aside conversions with RothC – calibration issues and uncertainty analysis

15 pages, 3 Figures and 3 Tables.

S1. Methods on physical fractionation and soil physicochemical analysis

The methodological approach was based on a physical fractionation scheme (Figure S2). Soils were separated in different water stable aggregate (WSA) fractions and the macro-aggregates were further separated in POM and smaller micro-aggregates. All fractions were measured for their content in C and N.

S1.1. Aggregate fractionation procedure

Bulk soil was gently sieved to pass through an 8 mm sieve and residual litter was removed. Then the soil was separated into five water stable aggregate (slake resistant) fractions according to the procedure based on Elliott (1986): i) large macro-aggregates (>2000 μm), ii) medium macro-aggregates (1000-2000 μm), iii) small macro-aggregates (250-1000 μm), iv) micro-aggregates (53-250 μm), and v) silt-clay sized micro-aggregates and minerals (<53 μm). Aggregate fractions were determined on triplicates, where air-dried soil (40 g) was quickly submerged in deionized water on top of the 2000 μm sieve (for 5 min), which was then moved up and down over 2 min with a stroke length of 3 cm for 50 strokes. The organic material floating on the water in the 2000 μm sieve was removed after the 2 min cycle because it is not considered SOM. Sieving was repeated on the 1000 μm (40 strokes), 250-μm (30 strokes) and 53-μm (10 strokes) sieves using the soil plus water that passed through the next larger sieve. Clay from the 53 μm sieve was gently removed. Aggregates remaining on each sieve were oven-dried at (40°C), weighed and stored in glass jars at room temperature. Sand content was determined on aggregate fraction subsamples after dispersing soil in sodium hexametaphosphate (0.5%) for 18 h on a rotary shaker at 190 rpm. The samples were then passed the sieve corresponded to the lower limit of each aggregate size (e.g the 1000-2000 μm sized aggregated with the 1000 μm sieve) and the sand mass retained in the sieve was used for sand correction. Mean weight diameter (MWD) was calculated by summing the weighted proportion of each aggregate fraction and was used as an index of aggregate stability.

S1.2. Micro-aggregate isolation procedure

In order to reveal possible differences in the composition and turnover rates of the macro-aggregates of different sizes and the patterns of the decomposition sequence the procedure was applied to both small macro-aggregates (250-1000 μm) and composite macro-aggregates (>250 μm) samples. A subsample (10 g) of small macro-aggregates (250-1000 μm) and of composite macro-aggregates (>250 μm) was further separated into the following fractions by the micro-aggregate isolation procedure outlined in Lichter et al., (2008): i) coarse particulate organic matter and sand (cPOM: >250 μm), ii) micro-aggregates (mM: 53-250 μm), and iii) easily dispersed silt-clay fractions (sc-M <53 μm). Briefly, the subsample of the aggregates was immersed in deionized water on top of a 250- mm mesh screen and gently shaken with 50 glass beads (4 mm in diameter) with continuous and steady water flow through the device to ensure that micro-aggregates were immediately flushed onto a 53-mm sieve and were not exposed to any further disruption by the beads (Six et al., 2000). After all macro-aggregates were broken up, the material on the 250 μm sieve was collected (cPOM) and on the 53-μm sieve was sieved to ensure that the isolated micro-aggregates were water stable (mM). The fraction that passed through the 53 μm sieve (sc-M) was also collected. The three fractions were oven-dried at (40°C), weighed and stored in glass jars at room temperature. The micro-aggregates within the macro-aggregates (mM) as well the 53-250 μm sized aggregates (micro-aggregates) were similarly separated to fine particulate organic matter and sand (fPOM: 53-250 μm) and silt-clay fraction of the micro-aggregate (sc-mM <53 μm). Using Lichter et al., (2008) as a guide, for this procedure we did not account for the separation of free POM and intra POM, as we observed that during the floatation procedure the macro-aggregates are collapsed and the separation cannot always be successful. Free POM which is also reported as occluded POM is negligible in terms of mass (1% and 2% for agricultural and forest soils respectively), but has the same C-to-N ratio as the free fraction (John et al., 2005).

S1.3. Physico-chemical analysis

Soils were measured for dry bulk density (gravimetric method), pH and soluble salts (conductivity)-measured in a 1:2 soil to water ratio (Methods of Soil Analysis, 1982), and texture (Bouyoucos, 1936). Additional soil analysis conducted by A&L Analytical Laboratories, Inc., Memphis, TN, included P, K, Ca, Mg, S, B, Cu, Fe, Mn, Zn, Na an Bicarb-P. The KCl extraction (2 mol L^{-1} KCl in a 1:5 soil-to-solution ratio) was used for the estimation of potential mineralizable N (PMN=NH3-N+NO3-N) of soils using a Hack 2010 spectrophotometer for NO_3-N (Cadmium Reduction Method, 8039) and NH_4-N (Salicylicate Method, 10023). Potential soluble organic nitrogen (PSON) was also measured by the Kjeldahl digestion technique (Nessler method, 8075). The potential soluble organic carbon (PSOC) was also estimated by a TOC analyzer (Shimadzu 5050), after the removal of inorganic carbon by air sparging for 10 min (Instruction Manual TOC-5050A, Shimadzu Corporation). The extracted pools were also measured for their content in carbohydrates colorimetrically using the phenol-sulfuric acid procedure (Piccolo et al., 1996). Bulk soil, aggregates, and fractions from the microaggregate isolation procedure were measured for their content in C by a TOC analyzer-solid sample module SSM-5000 (corrected for their inorganic C content) and N by the Kjeldahl digestion technique with a Hach digestahl digestion apparatus (Nessler method, 8075). The C and N content of the sc-mM fraction was not measured but estimated as the difference between the microaggregate (mM) and the fPOM.

References

Dale, R.F., 1968. The climatology of soil moisture, evaporation, and non-moistyre stress days for corn in Iowa. Agr. Meteorol. 5, 111-128.

Elliott, E.T., 1986. Aggregate structure and carbon, nitrogen, and phosphorus in native and cultivated soils. Soil Science Society of America Journal 50, 627-633.

Instruction Manual Total Organic Carbon Analyzer Model TOC-5050A, Shimadzu Corporation, Environmental Instrumental Division.

John, B., Yamashita, T., Ludwig, B., and Flessa, H., 2005. Storage of organic carbon in aggregate and density fractions of silty soils under different types of land use. Geoderma 128, 63-79.

Lichter, K., Govaerts, B., Six, J., Sayre, K.D., Deckers, J., Dendooven, L., 2008. Aggregation and C and N contents of soil organic matter fractions in a permanent raised-bed planting system in the highlands of Central Mexico. Plant and Soil 305, 237-252.

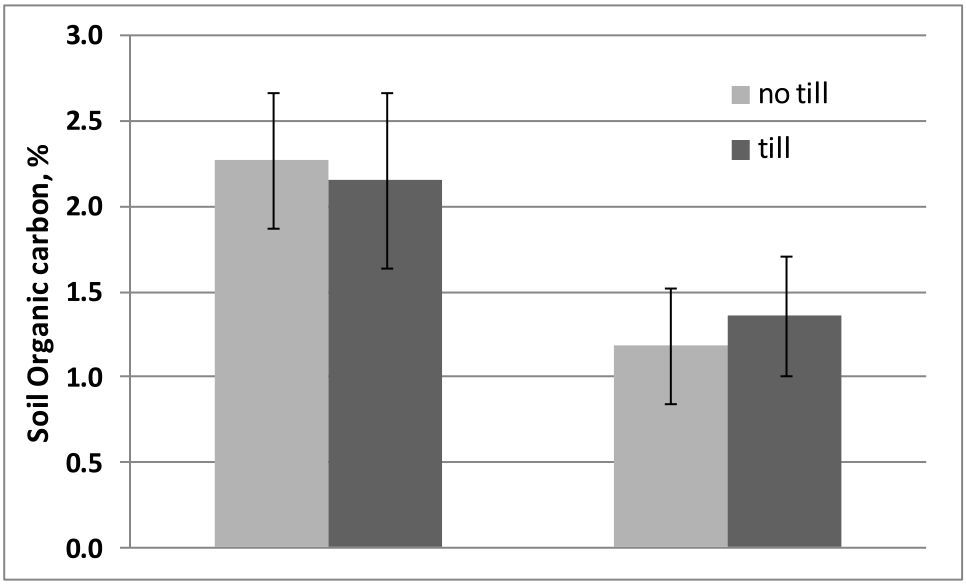

Fig. S1. Soil organic carbon content in topsoil (0-15 cm) and subsoil (15-30) of tilled and no-tilled olive groves fields (samples taken from the area between the trees) in the alluvial plain of Koiliaris River Basin (average and standard deviation derived by three spatial samples). Data taken from the 'soiltrec' project (www.soiltrec.eu) field campaign.

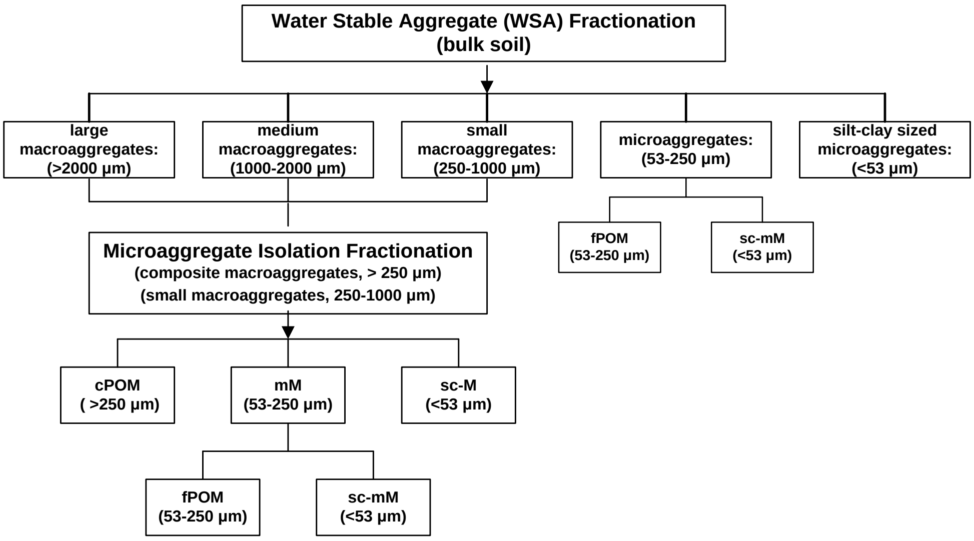

Fig. S2. Physical fractionation scheme used in the study. cPOM = coarse particulate organic matter, mM = micro-aggregates within macro-aggregates, sc-M = easily dispersed silt-clay fraction, fPOM = fine particulate organic matter, sc-mM = silt-clay fraction of the microaggregate.

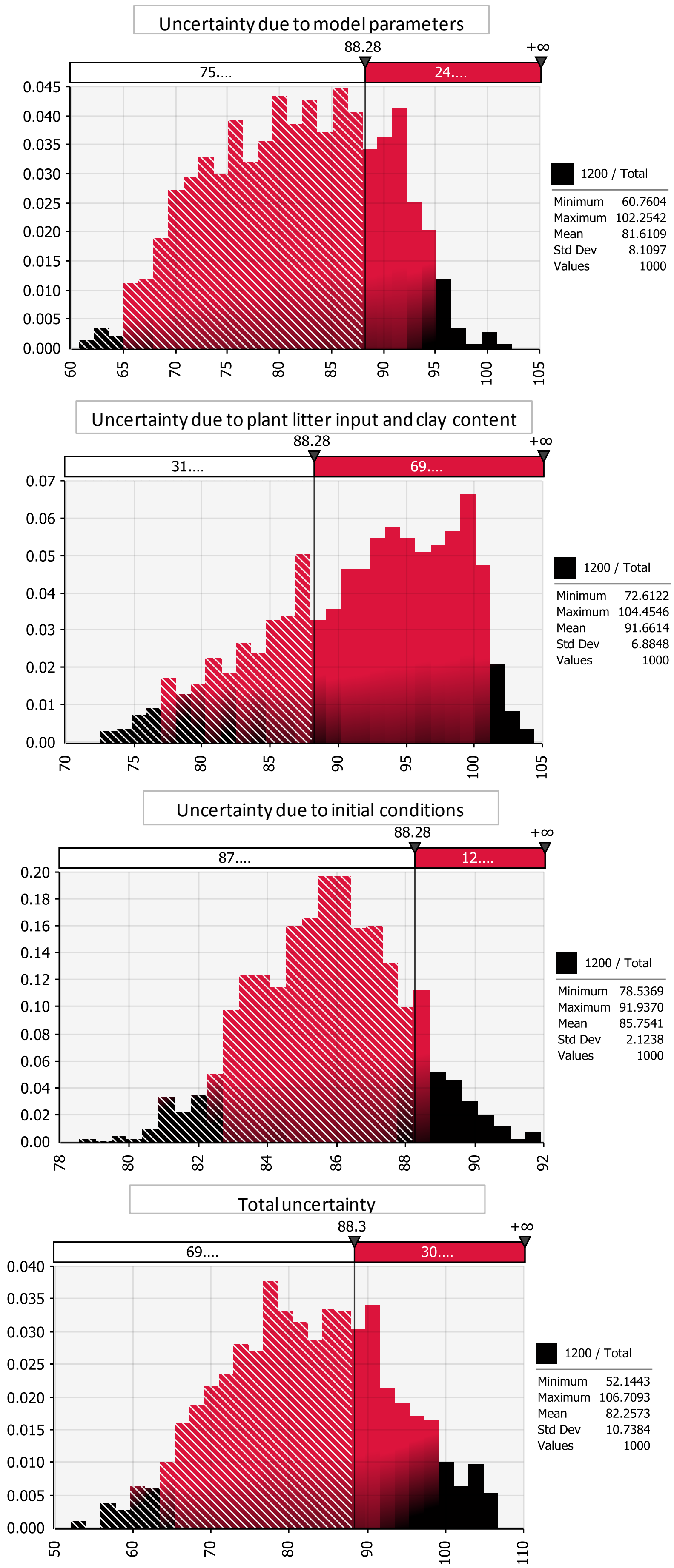
Uncertainty due to model parameters
88.28
+∞
75....
24....
1200 / Total
Minimum 60.7604
Maximum 102.2542
Mean 81.6109
Std Dev 8.1097
Values 1000
Uncertainty due to plant litter input and clay content
88.28
+∞
31....
69....
1200 / Total
Minimum 72.6122
Maximum 104.4546
Mean 91.6614
Std Dev 6.8848
Values 1000
Uncertainty due to initial conditions
88.28
+∞
87....
12....
1200 / Total
Minimum 78.5369
Maximum 91.9370
Mean 85.7541
Std Dev 2.1238
Values 1000
Total uncertainty
88.3
+∞
69....
30....
1200 / Total
Minimum 52.1443
Maximum 106.7093
Mean 82.2573
Std Dev 10.7384
Values 1000

(a)

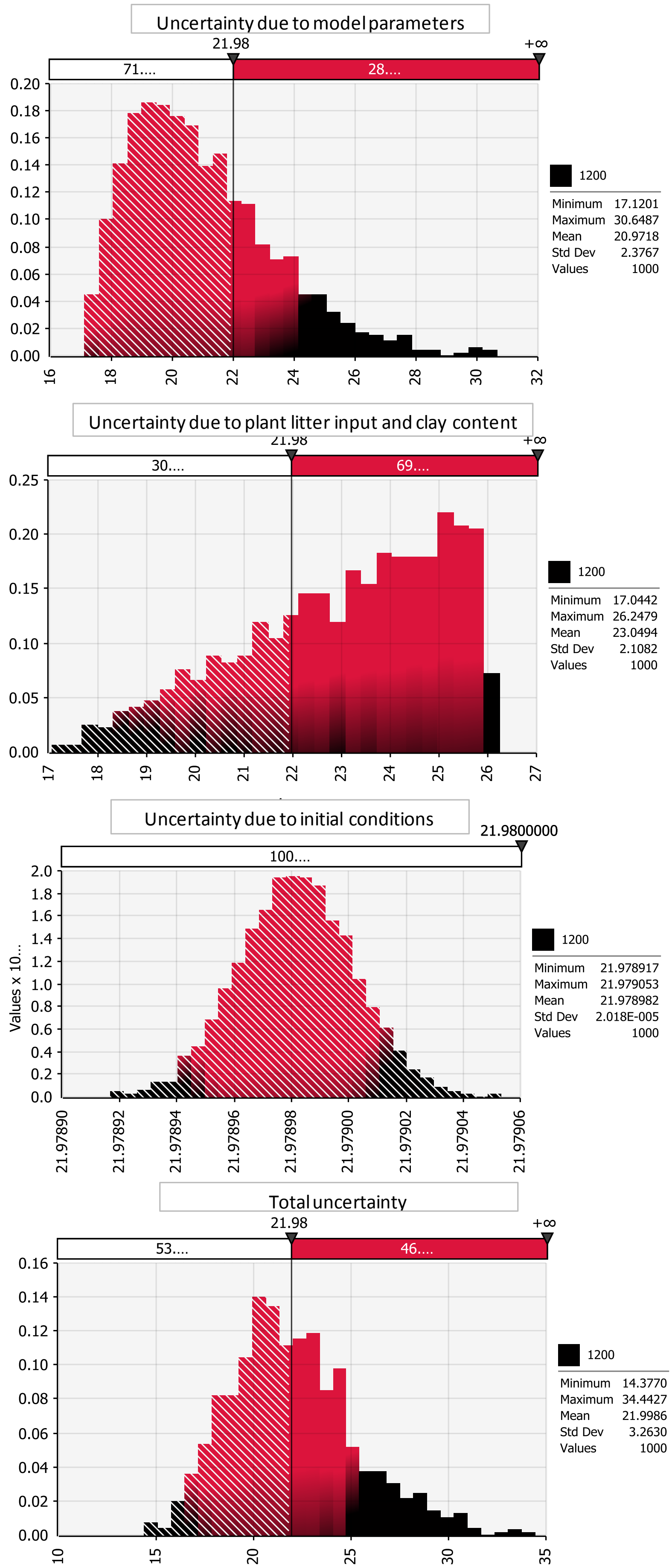

Uncertainty due to model parameters
21.98
+∞
71....
28....
1200
Minimum 17.1201
Maximum 30.6487
Mean 20.9718
Std Dev 2.3767
Values 1000
Uncertainty due to plant litter input and clay content
21.98
+∞
30....
69....
1200
Minimum 17.0442
Maximum 26.2479
Mean 23.0494
Std Dev 2.1082
Values 1000
Uncertainty due to initial conditions
21.9800000
100....
Values x 10...
1200
Minimum 21.978917
Maximum 21.979053
Mean 21.978982
Std Dev 2.018E-005
Values 1000
Total uncertainty
21.98
+∞
53....
46....
1200
Minimum 14.3770
Maximum 34.4427
Mean 21.9986
Std Dev 3.2630
Values 1000

(b)

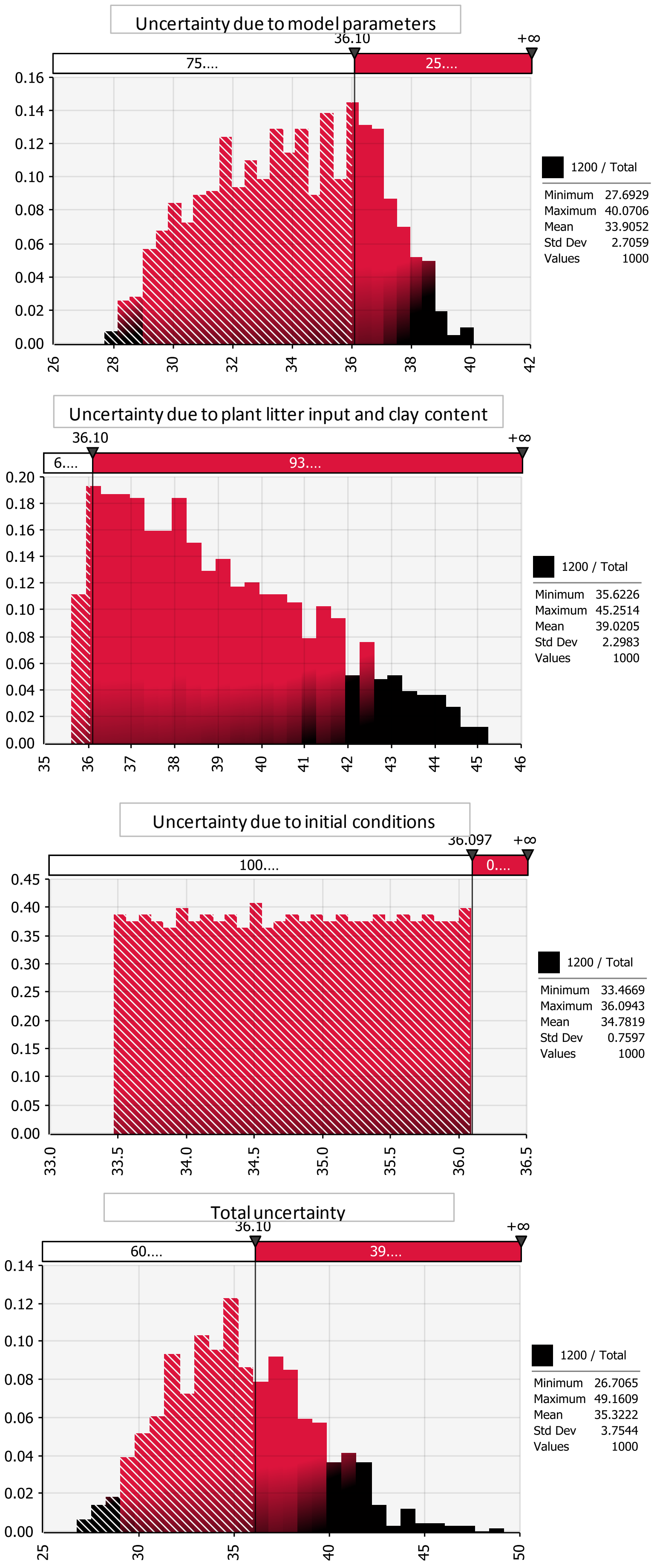

Uncertainty due to model parameters
1200 / Total
Minimum 27.6929
Maximum 40.0706
Mean 33.9052
Std Dev 2.7059
Values 1000
Uncertainty due to plant litter input and clay content
1200 / Total
Minimum 35.6226
Maximum 45.2514
Mean 39.0205
Std Dev 2.2983
Values 1000
Uncertainty due to initial conditions
1200 / Total
Minimum 33.4669
Maximum 36.0943
Mean 34.7819
Std Dev 0.7597
Values 1000
Total uncertainty
1200 / Total
Minimum 26.7065
Maximum 49.1609
Mean 35.3222
Std Dev 3.7544
Values 1000

(c)

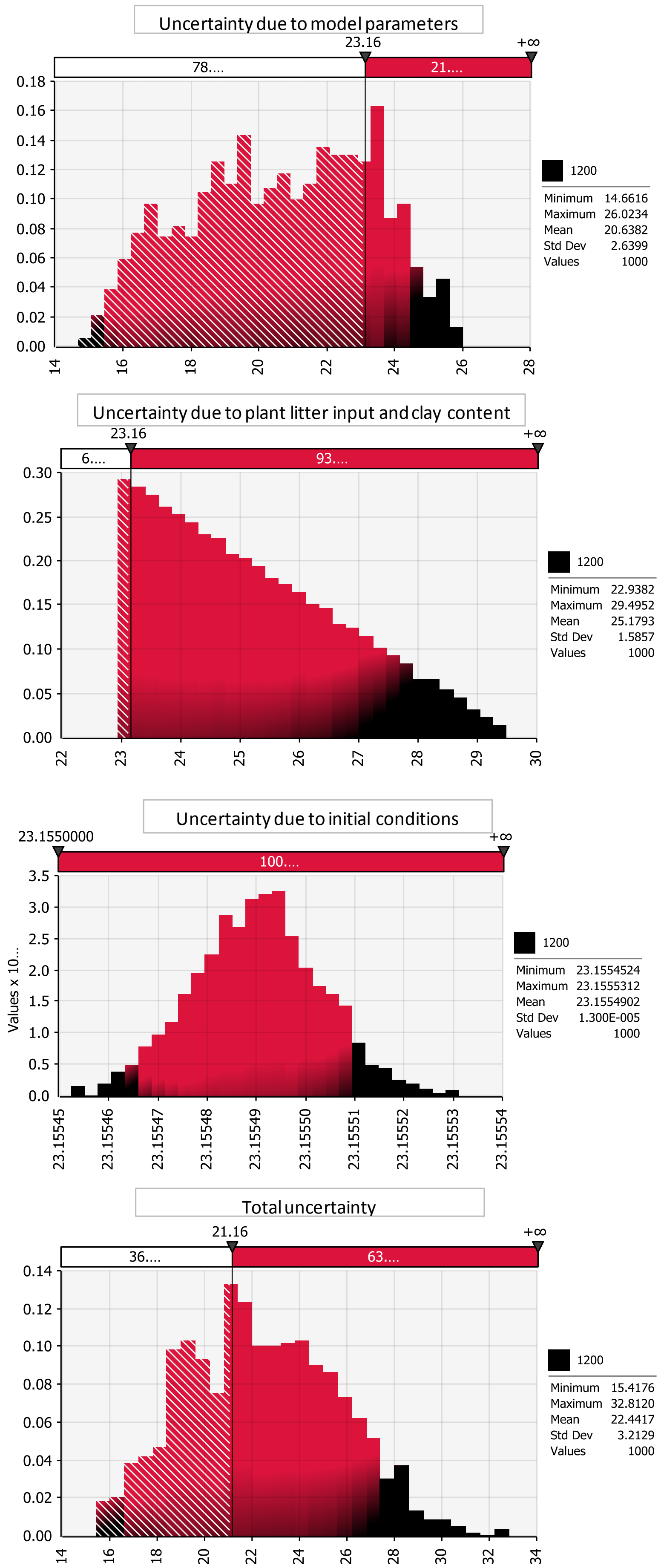
Uncertainty due to model parameters
23.16
+∞
78....
21....
1200
Minimum 14.6616
Maximum 26.0234
Mean 20.6382
Std Dev 2.6399
Values 1000
Uncertainty due to plant litter input and clay content
23.16
+∞
6....
93....
1200
Minimum 22.9382
Maximum 29.4952
Mean 25.1793
Std Dev 1.5857
Values 1000
Uncertainty due to initial conditions
23.1550000
+∞
100....
Values x 10...
1200
Minimum 23.1554524
Maximum 23.1555312
Mean 23.1554902
Std Dev 1.300E-005
Values 1000
Total uncertainty
21.16
+∞
36....
63....
1200
Minimum 15.4176
Maximum 32.8120
Mean 22.4417
Std Dev 3.2129
Values 1000

110

(d)

Fig. S2. The output distributions by the Monte-Carlo simulations for the calculation of the total uncertainty and uncertainty due to initial conditions, input data, and model parameters for 100 year of the simulation in Greece for a) SOC and b) POM and in Iowa for c) SOC and d) POM (the value of the optimum solution is indicated).

Table S1. Mean monthly meteorological data used for the application of the ROTHC model in the two sites (taken from the Local Climate Estimator-New LocClim 1.10, Grieser, 2006).

	IA (Iowa, USA)			**GR (Crete, Greece)**		
	Temperature	Precipitation	Potential evapotranspiration	Temperature	Precipitation	Potential evapotranspiration
January	-6	25	22	11	142	51
February	-4	24	27	11	112	57
March	3	60	55	13	81	80
April	11	94	96	16	32	112
May	17	103	133	20	13	159
June	22	115	160	24	5	203
July	25	125	165	26	1	222
August	23	112	143	26	2	199
September	19	99	108	23	19	142
October	13	72	82	19	80	94
November	5	54	45	16	73	64
December	-3	40	25	13	94	55
Annual	10	923	1060	18	652	1437

Table S2. Monthly and annual decomposition rates[a] (y^{-1}) for resistant plant material (RPM) and humus (HUM) soil organic pools pools of ROTHC model for the Greek and Iowa sites.

	IA (Iowa, USA)		**GR (Crete, Greece)**	
	RPM	HUM	RPM	HUM
January	0.001	0.001	0.152	0.003
February	0.008	0.006	0.157	0.003
March	0.073	0.059	0.039	0.001
April	0.248	0.201	0.051	0.001
May	0.093	0.075	0.070	0.001
June	0.132	0.107	0.091	0.002
July	0.151	0.123	0.101	0.002
August	0.140	0.114	0.098	0.002
September	0.105	0.085	0.085	0.002
October	0.061	0.049	0.066	0.001
November	0.092	0.075	0.161	0.003
December	0.008	0.007	0.186	0.004
Annual	0.093	0.075	0.105	0.002

[a]Decomposition rates constant multiplied by the rate modifying factor for temperature (a), the topsoil moisture deficit rate modifying factor (b), and the soil cover factor (c).

Table S3. Sensitivity coefficients (the absolute value of the ratio: (ΔY/Y)/(Δx/x)) for ROTHC model parameters for ±10% and ±50% change of the calibrated values for the Greek and Iowa sites.

	IA (Iowa, USA)				**GR (Crete, Greece)**			
prameter	(-50%)	(+50%)	(-10%)	(+10%)	(-50%)	(+50%)	(-10%)	(+10%)
total plant input	0.802	0.802	0.802	0.802	0.649	0.649	0.649	0.649
RPM[a]	0.460	0.272	0.365	0.329	0.504	0.207	0.329	0.276
DPM/RPM ratio[b]	0.425	0.228	0.316	0.280	0.154	0.102	0.128	0.118
HUM[c]	0.270	0.153	0.211	0.189	0.023	0.022	0.023	0.022
BIO%[d]	0.064	0.066	0.065	0.065	0.175	0.193	0.182	0.186
BIO[e]	0.099	0.045	0.069	0.059	0.042	0.014	0.024	0.019
DPM[f]	0.058	0.018	0.031	0.025	0.008	0.003	0.005	0.004

[a]Resistant plant material decomposition rate constant

[b]The apportionment ratio of Plant litter input between decomposable plant material (DPM) and RPM

[c]Humus decomposition rate constant

[d]The proportion that goes to BIO (100-BIO% is the proportion that goes to BIO)

[e]Biomass decomposition rate constant

[f]Decomposable plant material decomposition rate constant